

The *HST* Key Project on the Extragalactic Distance Scale XVII.

The Cepheid Distance to NGC 4725¹

Brad K. Gibson², Shaun M.G. Hughes³, Peter B. Stetson⁴, Wendy L. Freedman⁵, Robert C. Kennicutt, Jr.⁶, Jeremy R. Mould⁷, Fabio Bresolin⁸, Laura Ferrarese⁹, Holland C. Ford¹⁰, John A. Graham¹¹, Mingsheng Han¹², Paul Harding⁶, John G. Hoessel¹³, John P. Huchra¹⁴, Garth D. Illingworth¹⁵, Daniel D. Kelson¹¹, Lucas M. Macri¹⁴, Barry F. Madore¹⁶, Randy L. Phelps¹⁷, Charles F. Prosser^{18,19}, Abhijit Saha¹⁸, Shoko Sakai¹⁸, Kim M. Sebo⁷, Nancy A. Silbermann¹⁶ and Anne M. Turner⁶

¹Based on observations with the NASA/ESA *Hubble Space Telescope*, obtained at the Space Telescope Science Institute, which is operated by AURA, Inc., under NASA Contract No. NAS 5-26555.

Received _____; accepted _____

Submitted to ApJ, Part I

²Center for Astrophysics and Space Astronomy, University of Colorado, Campus Box 389, Boulder, CO, USA 80309

³Institute of Astronomy, Madingley Road., Cambridge, UK CB3 0HA

⁴Dominion Astrophysical Observatory, Herzberg Institute of Astrophysics, National Research Council, 5071 West Saanich Rd., Victoria, BC, Canada V8X 4M6

⁵The Observatories, Carnegie Institution of Washington, Pasadena, CA, USA 91101

⁶Steward Observatory, Univ. of Arizona, Tucson, AZ, USA 85721

⁷Mount Stromlo & Siding Spring Observatories, Australian National University, Weston Creek Post Office, Weston, ACT, Australia 2611

⁸European Southern Observatory, D-85748 Garching b. München, Germany

⁹Palomar Observatory, California Institute of Technology, Pasadena, CA, USA 91125

¹⁰Dept. of Physics & Astronomy, Bloomberg 501, Johns Hopkins Univ., 3400 N. Charles St., Baltimore, MD, USA 21218

¹¹Dept. of Terrestrial Magnetism, Carnegie Institution of Washington, 5241 Broad Branch Rd. N.W., Washington, D.C., USA 20015

¹²Avanti Corporation, 46871 Bayside Parkway, Fremont, CA, USA 94538

¹³Univ. of Wisconsin, Madison, WI, USA, 53706

¹⁴Harvard College, Center for Astrophysics, 60 Garden St., Cambridge, MA, USA 02138

¹⁵Lick Observatory, Univ. of California, Santa Cruz, CA, USA 95064

¹⁶Infrared Processing and Analysis Center, Jet Propulsion Laboratory, California Institute of Technology, Pasadena, CA, USA 91125

¹⁷Wright Laboratory of Physics, Oberlin College, 110 North Professor St., Oberlin, OH, USA 44074-1088

¹⁸National Optical Astronomy Observatories, P.O. Box 26732, Tucson, AZ, USA 85726

¹⁹Deceased

ABSTRACT

The distance to NGC 4725 has been derived from Cepheid variables, as part of the *Hubble Space Telescope Key Project on the Extragalactic Distance Scale*. Thirteen F555W (V) and four F814W (I) epochs of cosmic-ray-split Wide Field and Planetary Camera 2 observations were obtained. Twenty Cepheids were discovered, with periods ranging from 12 to 49 days. Adopting a Large Magellanic Cloud distance modulus and extinction of 18.50 ± 0.10 mag and $E(V-I)=0.13$ mag, respectively, a true reddening-corrected distance modulus (based on an analysis employing the ALLFRAME software package) of 30.50 ± 0.16 (random) ± 0.17 (systematic) mag was determined for NGC 4725. The corresponding distance of 12.6 ± 1.0 (random) ± 1.0 (systematic) Mpc is in excellent agreement with that found with an independent analysis based upon the DoPHOT photometry package. With a foreground reddening of only $E(V-I)=0.02$, the inferred *intrinsic* reddening of this field in NGC 4725, $E(V-I)=0.19$, makes it one of the most highly-reddened, encountered by the *HST Key Project*, to date.

Subject headings: Cepheids — distance scale — galaxies: distances and redshifts
— galaxies: individual (NGC 4725)

1. Introduction

The *Hubble Space Telescope (HST) Key Project on the Extragalactic Distance Scale* has as its primary goal the determination of the Hubble constant to an accuracy $\lesssim 10\%$ (Kennicutt, Freedman & Mould 1995). Cepheid distances to 18 spirals, within ~ 20 Mpc, are being obtained and will be used to calibrate a variety of secondary distance indicators, including the Tully-Fisher relation (TF), surface brightness fluctuations (SBF), planetary nebula luminosity function (PNLF), globular cluster luminosity function (GCLF), and Type Ia supernovae.

NGC 4725 is an Sb/SB(r)II barred spiral (Sandage 1996), with an uncorrected HI 21cm linewidth of ~ 411 km/s (Wevers et al. 1984), and an isophotal inclination of $\sim 46^\circ$ (de Vaucouleurs et al. 1991 - although, see Section 5.1). Its position ($\alpha = 12^{\text{h}}50^{\text{m}}27^{\text{s}}$, $\delta = +25^\circ30'06''$, J2000) and Galactocentric radial velocity $v = 1207$ km/s (de Vaucouleurs et al. 1991) led to its assignment to the Coma-Sculptor Cloud. NGC 4725 and 4747 are relatively isolated dynamically from the remainder of the Cloud (e.g. Zaritsky et al. 1997), and comprise what has come to be known as the Coma II Group of galaxies (e.g. Table II of Tully 1988). NGC 4725 is one of the *HST Key Project* primary calibrators for the infrared Tully-Fisher (IRTF) relationship. Because of the (assumed) association of the Coma II Group with that of the neighboring (larger) Coma I Group²⁰ (and, to some degree, the Coma-Sculptor Cloud as a whole), it was hoped that NGC 4725 would indirectly provide calibration for the SBF, PNLF, and GCLF secondary candles, a point to which we return in Section 5. NGC 4725 was the host galaxy for supernova SN1940B, a typical example of the “regular” class of “plateau” Type II events (Patat et al. 1994), but data do not exist which would allow application of the expanding photosphere method secondary distance indicator.

In Section 2 we present our multi-epoch Wide Field and Planetary Camera 2 (WFPC2) *HST* observations and review the two independent approaches taken to the photometry and calibration of the instrumental magnitudes – the methodology employed follows that of previous papers in this series (e.g. Stetson et al. 1998, and references therein). The identification of Cepheids and their derived properties, again employing two independent algorithms, are discussed in Section 3. The derived distance to NGC 4725 is presented in Section 4, and the result contrasted with previous distance determinations for NGC 4725 and the Coma I/II galaxy groups, in Section 5. A summary is provided in Section 6.

²⁰After Tully (1988), the Coma I Group is comprised of 25 members, including the notable elliptical NGC 4494 and edge-on spiral NGC 4565.

2. Observations and Photometry

HST WFPC2 observations of NGC 4725 were carried out over a two month period (1995 April 12 - 1995 June 14), with a single V epoch revisit on 1996 April 29. The revisit epoch, approximately one year after the conclusion of the main observing window, was used to constrain the periods of the longer-period Cepheids. In total, thirteen epochs of F555W (V), four epochs of F814W (I), and two epochs of F439W (B) were covered. Each epoch consisted of a pair of cosmic-ray-split exposures, each of duration 1000-1500 s. Because of the sparse phase coverage of the F439W observations and, more importantly, their insufficient signal-to-noise for detecting the majority of the Cepheid candidates, these were not included in the analysis which follows. The observing strategy, optimized to uncover Cepheids with periods $\sim 10 - 60$ days, follows that outlined in Freedman et al. (1994). The individual epochs, *HST* archive filenames, time at which a given epoch's observations began, and the exposure times and filters employed, are all listed in Table 1.

EDITOR: PLACE TABLE 1 HERE.

A $10' \times 10'$ ground-based image, obtained with the 2.5m Isaac Newton Telescope, is shown in Figure 1; the WFPC2 footprint has been superimposed. WFPC2 incorporates four 800×800 CCDs; the Planetary Camera (PC) has a 37×37 arcsecond field of view, and is referred to as Chip 1, while the three Wide Field Camera (WFC) chips have 80×80 arcsecond fields of view each, and are referred to as Chips 2, 3, and 4, respectively, moving counter-clockwise from the PC in Figure 1.

EDITOR: PLACE FIGURE 1 HERE.

As in previous papers in this series, dual independent analyses were undertaken using ALLFRAME (Stetson 1994) and DoPHOT (Saha et al. 1996, and references therein). As detailed descriptions of the reduction process can be found in Stetson et al. (1998), we only provide a brief summary of the key steps, in what follows.

2.1. ALLFRAME

The input star list to ALLFRAME was generated by median averaging the 26 F555W and 8 F814W cosmic-ray-split images of Table 1 to produce cosmic-ray-free frames for each chip/bandpass combination. Iterative application of DAOPHOT and ALLSTAR led to the

final master star list, which was input to ALLFRAME, and used to extract profile-fitting stellar photometry from the 34 individual frames. The adopted point spread functions (PSFs) were derived from public domain *HST* WFPC2 observations of the globular clusters Pal 4 and NGC 2419.

Aperture photometry was performed on the 45 isolated bright stars listed in Table 2. The program DAOGROW was then employed to generate growth curves out to $0''.5$, allowing an aperture correction to be derived for each chip and filter, to ensure a match to the Holtzmann et al. (1995) photometric system. The photometric zero points, aperture corrections, and long-exposure zero-point correction were then used to finally convert from instrumental magnitudes to the standard system, following the procedure outlined in Stetson et al. (1998).

EDITOR: PLACE TABLE 2 HERE.

2.2. DoPHOT

The DoPHOT philosophy concerning treatment of cosmic rays differs from that of ALLFRAME, in that each cosmic-ray-split pair was first combined using a sigma detection algorithm which takes into account the problems of undersampling (Saha et al. 1996). The final calibration of DoPHOT magnitudes follows that detailed in Section 2.2 of Stetson et al. (1998). Instrumental magnitudes were corrected to a $0''.5$ aperture magnitude using aperture corrections and zero points appropriate for long exposures, and converted to the standard system (Holtzmann et al. 1995). Calibrated DoPHOT photometry (and the associated error), for the 45 NGC 4725 reference stars, is listed in Table 2.

2.3. Comparison Between ALLFRAME and DoPHOT Photometry

A chip-by-chip comparison of ALLFRAME and DoPHOT photometry (both V- and I-bands) for the 45 reference stars of Table 2 is provided in Table 3. The agreement is very good for Chips 2-4 (i.e. the WFC fields), with a mean difference of -0.01 ± 0.07 mag in V, and -0.03 ± 0.07 mag in I, being determined (in the sense of ALLFRAME-DoPHOT). The largest single chip+filter discrepancy found is -0.07 ± 0.07 mag in I for Chip 4, which considering the 15 reference stars employed, is discrepant at the $\sim 4\sigma$ level. Such residual offsets have been observed in all *HST Key Project* galaxies to date; artificial star tests are currently underway, in order to ascertain and quantify the source of these discrepancies

(Ferrarese et al. 1999). Due to the absence of Cepheid candidates and bright reference stars in Chip 1 (i.e. the PC field), the comparison of Table 3 is restricted to Chips 2-4.

EDITOR: PLACE TABLE 3 HERE.

The comparison between ALLFRAME and DoPHOT mean magnitudes, for each of the 20 Cepheid candidates (detailed in Section 3), is likewise presented in Table 3. The mean differences of $+0.057 \pm 0.020$ mag in V, and $+0.016 \pm 0.017$ mag in I, are manifest in the slight offsets between the ALLFRAME and DoPHOT period-luminosity (PL) fits noted in Section 4.

3. Cepheid Identification

In a similar vein to the philosophy of performing dual independent photometric reductions with ALLFRAME and DoPHOT, independent Cepheid identification techniques were employed by each reduction team. Candidate Cepheids were extracted from the ALLFRAME dataset using TRIAL, Stetson’s (1996) template light curve fitting algorithm, whereas a variant of Stellingwerf’s (1978) phase dispersion minimization routine (Hughes 1989, and referred to as PDM henceforth) was adopted for the DoPHOT dataset.

Twenty high quality candidates were uncovered, the assigned identification numbers and coordinates (both (X,Y) on the respective WFC chip and (RA,DEC)) for which are listed in Table 4. The spatial distribution of the Cepheids in each chip is shown in Figure 2, with detailed ($4'' \times 4''$ windows centered upon each Cepheid) finding charts available in Figure 3.

EDITOR: PLACE TABLE 4 HERE.

EDITOR: PLACE FIGURE 2 HERE.

EDITOR: PLACE FIGURE 3 HERE.

The corresponding period and mean magnitude for each of the 20 Cepheids in question, as reported by TRIAL (for ALLFRAME data) and PDM (for DoPHOT data), is reproduced

(along with their accompanying errors) in Table 5; ALLFRAME light curves for each, phased to their respective period, are presented in Figure 4 - V- and I-band photometry represented by solid dots and open squares, respectively. The tabulated epoch-by-epoch ALLFRAME photometry (and associated errors), for each of the Cepheids, is given in Table 6. We have chosen to present all the photometry in Figure 4, including those epochs obviously affected by cosmic ray hits for Cepheids C04, C06, C08, C11, C12, and C17. It is important to stress though that the periods and mean magnitudes assigned by TRIAL and PDM have not been affected by these outliers, as clearly outlined by Stetson (1996) and Stetson et al. (1998).

EDITOR: PLACE TABLE 5 HERE.

EDITOR: PLACE FIGURE 4 HERE.

EDITOR: PLACE TABLE 6 HERE.

The 20 Cepheids listed in Table 5 have been identified in the deep V versus V–I color-magnitude diagram (CMD) of Figure 5; all clearly lie in the instability strip.

EDITOR: PLACE FIGURE 5 HERE.

4. The Distance to NGC 4725

As described previously by Ferrarese et al. (1996), the apparent V- and I-band distance moduli (i.e. μ_V and μ_I) to NGC 4725 are derived relative to that of the LMC, adopting Madore & Freedman’s (1991) LMC PL relations, scaled to a true modulus of $\mu_o = 18.50 \pm 0.10$ mag and reddening $E(V-I)=0.13$. In fitting to the NGC 4725 Cepheid data (Table 5), the slopes of the PL relations were fixed to those of Madore & Freedman’s LMC PL relations.

The ALLFRAME/DoPHOT V- and I-band PL relations for NGC 4725 are shown in Figures 6 and 7. The 20 Cepheids used in the final regression are denoted with solid circles, and listed in Table 5. The solid lines shown are the best fit regression, imposing the

LMC PL slopes, while the dotted lines represent 2σ deviations from the mean of the LMC relations (i.e. 0.54 mag in V, and 0.36 mag in I - Madore & Freedman 1991). The resulting apparent ALLFRAME distance moduli are $\mu_V = 31.00 \pm 0.06$ mag and $\mu_I = 30.80 \pm 0.06$ mag, with DoPHOT values of $\mu_V = 30.95 \pm 0.07$ mag and $\mu_I = 30.79 \pm 0.06$ mag. The 0.05 and 0.01 mag offsets in the apparent ALLFRAME and DoPHOT V-and I-band distance moduli, respectively, simply reflect the 0.057 and 0.016 mag Cepheid mean magnitude offsets presented in Section 2.3. The derived reddenings are $E(V-I)=0.21\pm 0.02$ (ALLFRAME) and $E(V-I)=0.16\pm 0.03$ (DoPHOT). The DIRBE/IRAS dust maps of Schlegel, Finkbeiner & Davis (1998) show a foreground reddening component of only $E(V-I)=0.02$ along this sight line; of the 19 galaxies examined by the *HST Key Project* to date, NGC 4725 possesses the greatest internal extinction.²¹

EDITOR: PLACE FIGURE 6 HERE.

EDITOR: PLACE FIGURE 7 HERE.

An independent estimate of the extinction internal to NGC 4725 can be obtained using the HI maps of Wevers et al. (1984), from which the HI surface density of the WFPC2 field is $\sim 6 \pm 2 \times 10^{20}$ atoms cm^{-2} . This range in HI column density should have associated with it enough dust to produce color excesses in the range $E(V-I)=0.03$ to 0.14, assuming a similar gas/dust ratio for NGC 4725 as for the low extinction regions of the Milky Way (i.e. equation 7 of Burstein & Heiles 1978). Our mean extinction for the Cepheids, although larger than this, is in reasonable agreement given the large uncertainties associated with gas-to-dust ratios, which in the Milky Way is reflected in the Heiles (1976) “R-parameter” (a useful measure of the total Galactic gas to dust ratio - see also equation 4 of Burstein & Heiles) ranging from -6 to +6, corresponding to a factor of 4 range in $dE(B-V)/dN_{\text{HI}}$ (Burstein & Heiles 1978).

Adopting a ratio of total to selective absorption of $A_V = 2.45 E(V - I)$, consistent with the Cardelli et al. (1989) extinction law, we derive true ALLFRAME and DoPHOT distance moduli of $\mu_o = 30.50 \pm 0.06$ mag and $\mu_o = 30.55 \pm 0.07$ mag, respectively, corresponding to

²¹Indeed, both NGC 4725 and 3621 are $2 \rightarrow 3\sigma$ outliers, in relation to the sample used by Kennicutt et al. (1998) to derive the relationship between Cepheid color excess and metallicity (i.e. $\delta E(V - I)/\delta[\text{O}/\text{H}] = 0.12 \pm 0.08$ mag/dex), in the sense of having higher excesses than expected for their metallicity.

$d = 12.6 \pm 0.4$ Mpc and $d = 12.9 \pm 0.4$ Mpc.²² Restricting ourselves to the 15 Cepheids with $P > 20$ d, as a test for incompleteness bias in the sample, the inferred distance moduli increase by 0.07 mag - an $\sim 1\sigma$ effect - allowing us to conclude that our results have not been severely compromised by such a bias.

The errors listed above reflect internal errors alone, arising from scatter in the NGC 4725 PL relations. A more complete assessment of the associated uncertainty, incorporating other potential random and systematic errors, is presented in Table 7. Uncertainties due to metallicity, LMC distance modulus, and photometric calibration all contribute to the NGC 4725 distance modulus error budget.

As in previous papers in this series (e.g. Hughes et al. 1998), the systematic uncertainty introduced by the adopted Cepheid PL calibration - ± 0.12 mag (S1 in Table 7) - is dominated by the error in the LMC true modulus (± 0.10 mag, from Madore & Freedman 1991 and Westerlund 1996).

The remaining systematic uncertainty in Table 7 which should be noted here is that due to a possible metallicity dependence of the Cepheid PL relation at V and I. Kennicutt et al. (1998), based upon two fields in M101, find a metallicity dependence of the form $d\mu_o/d[\text{O}/\text{H}] = -0.24 \pm 0.16$ mag/dex. If it can be shown that the NGC 4725 Cepheids differ substantially in metal abundance from those of the LMC Cepheids which calibrate the PL relation, a significant systematic error could be introduced into the derived distance.

Based upon 8 HII regions in NGC 4725, Zaritsky et al. (1994) determined a mean oxygen abundance of $12 + \log(\text{O}/\text{H}) = 9.26 \pm 0.57$, at a galactocentric distance $r = 3$ kpc, with a corresponding abundance gradient of -0.022 ± 0.063 dex/kpc. With the WFPC2 fields at a galactocentric distance of $\sim 13 \pm 2$ kpc (recall the $10' \times 10'$ scale of Figure 1), we therefore estimate a mean oxygen abundance for the fields of $12 + \log(\text{O}/\text{H}) \approx 9.0 \pm 0.3$. In contrast, the mean calibrating LMC HII region abundance used by the *HST Key Project* is $12 + \log(\text{O}/\text{H}) = 8.5$ (Kennicutt et al. 1998). Recalling the aforementioned Kennicutt et al. Cepheid metallicity dependence, this possible factor of three greater Cepheid metallicity in NGC 4725, in comparison with the LMC Cepheids, could cause the Cepheid distance modulus to NGC 4725 to be underestimated by $\sim 0.12 \pm 0.21$ mag. In keeping with

²²The PL fitting methodology adopted in the current study is identical to that adopted throughout the *HST Key Project* series - i.e. the absolute distance modulus μ_o , associated reddening $E(V-I)$, and their associated uncertainties, are derived directly from the full sample of 20 individually de-reddened Cepheids, and not indirectly through a comparison of the apparent distance moduli (μ_V and μ_I).

earlier papers in this series, and noting the large uncertainty attached to the metallicity extrapolation for our Cepheid field, this potential correction to the distance modulus of $+0.12 \pm 0.21$ mag is not currently applied, but simply added to the appropriate systematic error budget in Table 7. We will revisit the issue of the effects of metallicity on distances to *HST Key Project* galaxies in a consistent manner when all of the measurements of galaxy distances in our sample have been completed.

In light of the complete list of random and systematic errors shown in Table 7, our final quoted Cepheid-based true distance moduli to NGC 4725 are $\mu_o = 30.50 \pm 0.16$ (random) ± 0.17 (systematic) mag (ALLFRAME) and $\mu_o = 30.55 \pm 0.16$ (random) ± 0.17 (systematic) mag (DoPHOT), with reddenings of $E(V-I)=0.21\pm0.02$ (internal) and $E(V-I)=0.16\pm0.03$ (internal), respectively. The corresponding distances are 12.6 ± 1.0 (random) ± 1.0 (systematic) Mpc (ALLFRAME) and 12.9 ± 1.0 (random) ± 1.0 (systematic) Mpc (DoPHOT).

5. Previous Distance Determinations for NGC 4725 and the Coma Cloud

Previous distance determinations for NGC 4725 have been based upon either measurements of NGC 4725 itself, or indirectly through an assumed association with the Coma I or II Groups, within the Coma-Sculptor Cloud. Table 8 provides a summary of both families of distance determinations. The method employed is noted in column 1, the distance and quoted error (both in Mpc) in column 2, and the appropriate reference in column 3. Again, Tully’s (1988) Coma Cloud inventory has been adopted in Table 8; while convenient, this should *not* be construed as unequivocal support for any assumed physical association between these tabulated galaxies.

EDITOR: PLACE TABLE 8 HERE.

Early quoted values for NGC 4725 proper include Bottinelli et al.’s (1985) B-band Tully-Fisher (TF)-derived value of $d = 9.9 \pm 1.0$ Mpc and Tully’s (1988) $d = 12.4$ Mpc, derived from assuming $H_o = 75$ km/s/Mpc, along with a simple Virgocentric flow model. Subsequent to this, and adopting an H-band TF relationship zero-point tied to M31, M33, and NGC 2403, Tully et al. (1992) found $d = 16.1$ Mpc.²³ Tully (1997) has since revised

²³Note, though, that the predicted distance output from their mass model of the same paper (Tully et al. 1992) was 20 Mpc, symptomatic of the well-documented “triple-value ambiguity”, discussed therein.

the TF distance to NGC 4725, by taking into account not only the H band, but also B-, R-, and I-bands, the average of which yields 12.6 ± 2.1 Mpc, in agreement with our Cepheid distance of 12.6 ± 1.0 (random) ± 1.0 (systematic) Mpc.

NGC 4725 is one of only 6 spirals for which a *direct* comparison between SBF- and either maser- or Cepheid-derived distances can be made (the others being NGC 224, 3031, 3368, 4258, and 7331). Tonry’s (1998) interim SBF distance to the bulge of NGC 4725 of 13.1 ± 2.2 Mpc, likewise agrees with our newly-derived Cepheid distance.²⁴ The SBF Survey is currently undergoing final recalibration (Tonry 1998), at which time the definitive comparison can be made.

The range of direct and indirect distance determinations to galaxies generally associated with the classical Coma Groups I and II (ie 10-19 Mpc), as reflected by the compilation of Table 8, reinforces the conclusions of Turner et al. (1998, Section 7) regarding the limited use of these two galaxy groups for calibrating secondary distance indicators.

5.1. Infrared Tully-Fisher Relationship

The interim H-band Tully-Fisher relation, derived from the 19 calibrators currently available, is shown in Figure 8, and follows that given by Mould et al. (1997). The Aaronson et al. (1982) H-band photometric index $H_{-0.5}$, coupled with the 21cm linewidths tabulated by Tormen & Burstein (1995), were employed. For comparison, Freedman’s (1990) earlier IRTF calibration, based upon only 5 local calibrators, is shown. The 0.47 magnitude offset between the two calibrations can be traced to the sample of five galaxies available to Freedman in 1990; *each* of these five (NGC 224, 300, 598, 2403, and 3031) are $\sim 0.2 \rightarrow 0.5$ mag fainter in $H_{-0.5}$ than the mean global values found for expected for their respective HI linewidths. This only becomes apparent when the entire sample of 19 IRTF calibrators is considered.

²⁴Tonry’s (1998) interim distance to the bulge of NGC 4725 (i.e. 13.1 ± 2.2 Mpc) supersedes the earlier *indirect* SBF measurement to the Coma II Group of galaxies of 15.9 ± 0.6 Mpc (Tonry et al. 1997). The latter was based upon an assumed association with NGC 4494 and 4565, an assumption no longer necessary with the now available *direct* SBF distance determination. As recognized by Tonry et al., the disagreement between SBF and PNLF/GCLF distances to NGC 4494 and 4565 (Fleming et al. 1995; Forbes 1996; Jacoby et al. 1996) still remains unresolved, and is reflected in the relevant entries to Table 8.

EDITOR: PLACE FIGURE 8 HERE.

The subject of this paper, NGC 4725, identified in Figure 8 by the open circle, possesses an H-band luminosity a factor of two lower than expected for its linewidth (similar to NGC 224≡M31). While we do not wish to belabor or overinterpret this mild divergence ($< 1\sigma$) from the mean Tully-Fisher relation, there are several points which should be made. It is apparent that NGC 4725 and its neighbor NGC 4747 (at a projected distance of ~ 88 kpc) have undergone a past encounter. The striking ~ 50 kpc-long HI plumes extending from the center of NGC 4747, including the one pointed directly at NGC 4725, clearly support this picture (Wevers et al. 1984). Given that NGC 4725 is twenty times as massive as NGC 4747, it is not surprising to find that while the latter is severely distorted, the former is far more stable against tidal interactions and only shows a minor elongation and possible warping of the outer south-eastern spiral arm. Still, a consequence of this distorted spiral arm is that the outer isophotes are less elongated than the inner ones, which may lead to an underestimate of the inclination should it be based solely on the outer isophotes. This may be the source of the mild discrepancy between the photometric inclination of 46° (de Vaucouleurs et al. 1991) and the outer disk HI kinematic inclination of 53° (Wevers et al. 1984), although it should be stressed that the values are consistent within the quoted errors ($\pm 4^\circ$). We note in passing that increasing the assumed inclination from 46° to 53° will have the effect of shifting the $\log(\Delta V)$ for NGC 4725 in Figure 8 from 2.76 to 2.71, eliminating its $\sim 1\sigma$ outlier status from the mean IRTF relation. Such issues will be addressed fully in the *HST Key Project's* Tully-Fisher calibration paper (Sakai et al. 1998); for the time being though, we retain complete self-consistency with the compiled H-band magnitudes and 21cm linewidths in Tormen & Burstein (1995).

6. Summary

HST WFPC2 imaging of the Coma II group galaxy NGC 4725 has led to the discovery of twenty Cepheids with periods ranging from 12 to 49 days. Based upon the resultant V- and I-band period-luminosity relations, we obtained true distance moduli of 30.50 ± 0.16 (random) ± 0.17 (systematic) and 30.55 ± 0.16 (random) ± 0.17 (systematic) mags, and reddenings of $E(V-I) = 0.21 \pm 0.02$ (internal) and 0.16 ± 0.03 (internal) mags, for the ALLFRAME- and DoPHOT-reduced datasets, respectively. The corresponding distances are then 12.6 ± 1.0 (random) ± 1.0 (systematic) and 12.9 ± 1.0 (random) ± 1.0 (systematic) Mpc, in excellent agreement with the most recent Tully-Fisher (Tully 1997) and SBF (Tonry 1998) distances to NGC 4725. While useful as a calibrator for these two secondary distance indicators, we echo the conclusions of Turner et al. (1998) in that our Cepheid-

derived distance is of limited use for calibrating secondary indicators pertaining to the Coma-Sculptor Cloud proper.

The work presented in this paper is based on observations with the NASA/ESA Hubble Space Telescope, obtained by the Space Telescope Science Institute, which is operated by AURA, Inc. under NASA contract No. 5-26555. The continued assistance of the NASA and STScI support staff, and in particular our program coordinator, Doug Van Orsow, is gratefully acknowledged. Support for this work was provided by NASA through grant GO-2227-87A from STScI. SMGH and PSB are grateful to NATO for travel support via a Collaborative Research Grant (960178). We wish to thank John Tonry, Brent Tully, Bill Harris, and Robin Ciardullo, for many enlightening correspondences.

REFERENCES

- Aaronson, M., et al. 1982, *ApJS*, 50, 241
- Bottinelli, L., Gouguenheim, L., Paturel, G. & de Vaucouleurs, G. 1985, *A&AS*, 59, 43
- Burstein, D. & Heiles, C. 1978, *ApJ*, 225, 40
- Cardelli, J.A., Clayton, G.C. & Mathis, J.S. 1989, *ApJ*, 345, 245
- de Vaucouleurs, G., de Vaucouleurs, A., Corwin, H., Buta, R., Paturel, A. & Fouqué, P. 1991, *Third Reference Catalogue of Bright Galaxies* (Berlin: Springer) ESA SP-310
- Ferrarese, L., et al. 1996, *ApJ*, 464, 568
- Ferrarese, L., et al. 1999, *ApJ*, in preparation
- Fleming, D.E.B., Harris, W.E., Pritchett, C.J. & Danes, D.A. 1995, *AJ*, 109, 1044
- Forbes, D.A. 1996, *AJ*, 112, 1409
- Freedman, W.L. 1990, *ApJ*, 355, 35
- Freedman, W.L., et al. 1994, *ApJ*, 427, 628
- Heiles, C. 1976, *ApJ*, 204, 379
- Holtzmann, J.A., et al. 1995, *PASP*, 107, 1065
- Hughes, S.M.G. 1989, *AJ*, 97, 1634
- Hughes, S.M.G., et al. 1998, *ApJ*, 501, 32
- Jacoby, G.H., Ciardullo, R. & Harris, W.E. 1996, *ApJ*, 462, 1
- Kennicutt, Jr., R.C., Freedman, W.L. & Mould, J.R. 1995, *AJ*, 110, 1476
- Kennicutt, Jr., R.C., et al. 1998, *ApJ*, 498, 181
- Madore, B.F. & Freedman, W.L. 1991, *PASP*, 103, 933
- Mould, J.R., Sakai, S., Hughes, S. & Han, M. 1997, in Livio, M., Donahue, M. & Panagia, N., eds, *The Extragalactic Distance Scale*, Cambridge Univ Press, Cambridge, p. 158
- Patat, F., Barbon, R., Cappellaro, E. & Turatto, M. 1994, *A&A*, 282, 731

- Saha, A., Sandage, A., Labhardt, L., Tammann, G.A., Maccetto, F.D. & Panagia, N. 1996, ApJ, 466, 55
- Sakai, S., et al. 1998, ApJ, in preparation
- Sandage, A. 1996, AJ, 111, 18
- Schlegel, D.J., Finkbeiner, D.P. & Davis, M. 1998, ApJ, 500, 525
- Simard, L. & Pritchett, C.J. 1994, AJ, 107, 503
- Stellingwerf, R.F. 1978, ApJ, 224, 953
- Stetson, P.B. 1994, AJ, 106, 205
- Stetson, P.B. 1996, PASP, 108, 851
- Stetson, P.B., et al. 1998, ApJ, in press
- Tonry, J.L. 1998, priv comm
- Tonry, J.L., Blakeslee, J.P., Ajhar, E.A. & Dressler, A. 1997, ApJ, 475, 399
- Tormen, G. & Burstein, D. 1995, ApJS, 96, 123
- Tully, R.B. 1988, Nearby Galaxies Catalog (Cambridge: Cambridge University Press)
- Tully, R.B. 1997, priv comm
- Tully, R.B. & Shaya, E.J. 1984, ApJ, 281, 31
- Tully, R.B., Shaya, E.J. & Pierce, M.J. 1992, ApJS, 80, 479
- Turner, A., et al. 1998, ApJ, in press
- Westerlund, B.E. 1996, The Magellanic Clouds, Cambridge Univ Press, Cambridge
- Wevers, B.M.H.R., Appleton, P.N., Davies, R.D. & Hart, L. 1984, A&A, 140, 125
- Zaritsky, D., Kennicutt, Jr., R.C. & Huchra, J.P. 1994, ApJ, 420, 87
- Zaritsky, D., Smith, R., Frenk, C. & White, S.D.M. 1997, ApJ, 478, 39

Fig. 1.— A $10' \times 10'$ ground-based image of NGC 4725, taken at the 2.5m Isaac Newton Telescope. North is to the top and east to the left. The WFPC2 footprint is superimposed, where C1 represents the Planetary Camera chip, and C2, C3, and C4 the Wide Field Camera chips. **See accompanying jpg file: f1.jpg**

Fig. 2.— (a) The $80'' \times 80''$ field of view of the WFC Chip 2 in NGC 4725. North is toward the left, east to the bottom. Locations of the Cepheid candidates are marked, with detailed finding charts available for each in Figure 3. (b) The $80'' \times 80''$ field of view of the WFC Chip 3 in NGC 4725. North is toward the top, east to the left. Locations of the Cepheid candidates are marked, with detailed finding charts available for each in Figure 3. (c) The $80'' \times 80''$ field of view of the WFC Chip 4 in NGC 4725. North is toward the right, east to the top. Locations of the Cepheid candidates are marked, with detailed finding charts available for each in Figure 3. **See accompanying jpg files: f2a.jpg - f2c.jpg**

Fig. 3.— Finder charts for each of the Cepheid candidates for NGC 4725. Each image is 41×41 pixels (i.e. $4'' \times 4''$), with an orientation matching that of Figure 2. In each case, the Cepheid is situated at the exact center of the panel. **See accompanying jpg file: f3.jpg**

Fig. 4.— Calibrated ALLFRAME V- (filled circles) and I-band (open squares) phased lightcurves (two cycles), for the Cepheids listed in Table 4. All data from Table 6 are shown, including obvious cosmic-ray-affected epochs in the lightcurves of Cepheids C04, C06, C08, C11, C12, and C17. Said cosmic-ray hits do not impact upon the period determination (Stetson 1996), but are shown for completeness. **See accompanying jpg files: f4a.jpg - f4d.jpg**

Fig. 5.— Calibrated ALLFRAME photometry (V,V–I) color-magnitude diagram for the three WFC chips. The filled circles represent the 20 NGC 4725 Cepheid candidates of Table 4.

Fig. 6.— Period-luminosity relations in the V (top panel) and I (bottom panel) bands, based on the calibrated ALLFRAME photometry. The filled circles represent the 20 high-quality NGC 4725 Cepheid candidates found by TRIAL (see Tables 4 and 5). The solid lines are least squares fits, with the slope fixed to be that of the Madore & Freedman (1991) LMC PL-relations, while the dotted lines represent their corresponding 2σ dispersion. The inferred apparent distance moduli are then $\mu_V = 31.00 \pm 0.06$ mag (internal) and $\mu_I = 30.80 \pm 0.06$ mag (internal).

Fig. 7.— Period-luminosity relations in the V (top panel) and I (bottom panel) bands, based on the calibrated DoPHOT photometry. The filled circles represent the 20 high-quality NGC 4725 Cepheid candidates found by PDM (see Tables 4 and 5). The solid lines

are least squares fits, with the slope fixed to be that of the Madore & Freedman (1991) LMC PL-relations, while the dotted lines represent their corresponding 2σ dispersion. The inferred apparent distance moduli are then $\mu_V = 30.91 \pm 0.07$ mag (internal) and $\mu_I = 30.76 \pm 0.06$ mag (internal).

Fig. 8.— IRTF absolute calibration, with absolute $H_{-0.5}$ magnitudes versus HI linewidth $\log(\Delta V)$, from Aaronson et al. (1982) and Tormen & Burstein (1995), respectively. The interim calibration (represented by the solid curve) parallels that of Mould et al. (1997), and is based upon the available sample of 19 calibrators with Cepheid-derived distances. The dashed curve is Freedman’s (1990) calibration, based upon 5 local calibrators. The circled dot represents NGC 4725.

Table 1. HST Observations of NGC 4725

Epoch	Filename	Date	Julian Date	Exposure Times (s)		Filter
1	u2782j01t/2t	12/04/95	2449819.813	1500	1000	F555W
2	u2782k01t/2t	21/04/95	2449828.528	1500	1000	F555W
3	u2782l01t/2t	02/05/95	2449839.777	1500	1000	F555W
4	u2782m01t/2t	05/05/95	2449842.722	1500	1000	F555W
5	u2782n01t/2t	07/05/95	2449845.269	1500	1000	F555W
6	u2782o01t/2t	11/05/95	2449848.756	1500	1000	F555W
7	u2782p01t/2t	15/05/95	2449852.993	1500	1000	F555W
8	u2782q01t/2t	19/05/95	2449856.946	1500	1000	F555W
9	u2782r01p/2p	24/05/95	2449862.174	1500	1000	F555W
10	u2782s01p/2p	30/05/95	2449868.206	1500	1000	F555W
11	u2782t01t/2t	06/06/95	2449874.974	1500	1000	F555W
12	u2782u01t/2t	14/06/95	2449883.417	1500	1000	F555W
13	u2s76001t/2t	29/04/96	2450203.095	1100	1100	F555W
2	u2782k03t/4t	21/04/95	2449828.593	1000	1500	F814W
3	u2782l03t/4t	02/05/95	2449839.850	1000	1500	F814W
8	u2782q03t/4t	19/05/95	2449857.013	1000	1500	F814W
12	u2782u03t/4t	14/06/95	2449883.482	1000	1500	F814W
3	u2782l05t/6t	02/05/95	2449839.973	1500	1000	F439W
8	u2782q08t/9t	19/05/95	2449857.149	1300	1200	F439W

Table 2. Reference Star Photometry.

ID	Chip	X	Y	RA (J2000)	Dec	ALLFRAME		DoPHOT	
						V	I	V	I
R01	2	721.2	210.7	12:50:35.44	25:31:41.8	24.23 ± 0.01	22.40 ± 0.01	24.11 ± 0.02	22.42 ± 0.02
R02	2	107.7	214.5	12:50:35.78	25:32:42.7	24.08 ± 0.01	22.11 ± 0.01	24.01 ± 0.02	22.03 ± 0.01
R03	2	451.8	258.5	12:50:35.25	25:32:08.9	23.97 ± 0.01	23.94 ± 0.03	23.95 ± 0.02	23.86 ± 0.03
R04	2	684.3	278.6	12:50:34.96	25:31:46.0	23.97 ± 0.01	23.76 ± 0.03	24.01 ± 0.02	23.79 ± 0.02
R05	2	155.4	291.7	12:50:35.18	25:32:38.6	24.24 ± 0.01	23.89 ± 0.03	24.20 ± 0.02	23.84 ± 0.05
R06	2	150.3	322.9	12:50:34.96	25:32:39.3	23.53 ± 0.01	23.19 ± 0.02	23.50 ± 0.01	23.20 ± 0.05
R07	2	791.9	344.7	12:50:34.41	25 31:35.9	23.09 ± 0.01	22.82 ± 0.02	23.13 ± 0.02	22.87 ± 0.03
R08	2	613.1	351.9	12:50:34.47	25:31:53.7	23.02 ± 0.01	21.90 ± 0.01	23.08 ± 0.01	21.95 ± 0.02
R09	2	631.3	360.8	12:50:34.39	25:31:51.9	22.78 ± 0.02	22.55 ± 0.01	22.89 ± 0.01	22.57 ± 0.01
R10	2	414.3	463.4	12:50:33.77	25:32:14.3	23.07 ± 0.01	22.94 ± 0.02	23.03 ± 0.03	22.98 ± 0.02
R11	2	105.5	533.9	12:50:33.44	25:32:45.5	24.12 ± 0.01	24.12 ± 0.03	23.92 ± 0.03	24.03 ± 0.05
R12	2	84.2	605.4	12:50:32.92	25:32:48.2	22.42 ± 0.01	22.06 ± 0.01	22.44 ± 0.02	21.97 ± 0.06
R13	2	81.5	624.7	12:50:32.78	25:32:48.6	23.34 ± 0.01	23.06 ± 0.02	23.36 ± 0.02	23.06 ± 0.03
R14	2	178.6	653.5	12:50:32.51	25:32:39.2	23.52 ± 0.01	23.02 ± 0.02	23.46 ± 0.02	22.98 ± 0.01
R15	2	377.2	673.5	12:50:32.25	25:32:19.7	24.51 ± 0.02	23.44 ± 0.04	24.54 ± 0.02	23.41 ± 0.03
R16	2	193.4	680.6	12:50:32.31	25:32:38.0	24.17 ± 0.01	21.61 ± 0.01	24.06 ± 0.03	21.54 ± 0.03
R17	2	344.4	680.7	12:50:32.22	25:32:23.0	24.41 ± 0.01	24.37 ± 0.05	24.40 ± 0.02	24.39 ± 0.03
R18	3	378.9	225.0	12:50:34.77	25:33:07.4	23.44 ± 0.01	22.95 ± 0.02	23.53 ± 0.03	23.05 ± 0.02
R19	3	445.5	240.4	12:50:34.29	25:33:09.5	23.87 ± 0.01	23.83 ± 0.03	23.92 ± 0.03	23.84 ± 0.02
R20	3	445.1	269.2	12:50:34.31	25:33:12.3	23.48 ± 0.01	23.44 ± 0.02	23.58 ± 0.07	23.46 ± 0.01
R21	3	642.8	272.0	12:50:32.87	25:33:14.3	23.82 ± 0.01	23.67 ± 0.03	23.88 ± 0.03	23.70 ± 0.03
R22	3	184.4	286.8	12:50:36.24	25:33:11.8	24.23 ± 0.01	22.83 ± 0.02	24.28 ± 0.02	22.84 ± 0.03
R23	3	648.7	354.7	12:50:32.88	25:33:22.6	22.71 ± 0.01	22.42 ± 0.01	22.80 ± 0.01	22.51 ± 0.02
R24	3	265.5	493.9	12:50:35.77	25:33:33.1	24.10 ± 0.01	23.86 ± 0.03	24.12 ± 0.03	23.88 ± 0.02
R25	3	528.1	500.0	12:50:33.85	25:33:35.9	24.36 ± 0.01	23.96 ± 0.04	24.41 ± 0.02	24.05 ± 0.01
R26	3	456.9	544.3	12:50:34.40	25:33:39.7	22.63 ± 0.01	22.10 ± 0.01	22.68 ± 0.01	22.14 ± 0.03
R27	3	394.3	547.2	12:50:34.86	25:33:39.5	24.08 ± 0.01	24.07 ± 0.03	24.11 ± 0.01	24.00 ± 0.04
R28	3	473.7	568.4	12:50:34.30	25:33:42.2	23.44 ± 0.01	23.50 ± 0.02	23.48 ± 0.02	23.52 ± 0.02
R29	3	602.5	697.2	12:50:33.43	25:33:56.1	23.57 ± 0.01	23.31 ± 0.02	23.58 ± 0.01	23.32 ± 0.01
R30	3	494.7	767.5	12:50:34.27	25:34:02.2	24.00 ± 0.01	23.93 ± 0.03	23.95 ± 0.04	23.95 ± 0.02
R31	4	210.1	148.3	12:50:38.04	25:33:02.1	24.23 ± 0.01	22.75 ± 0.04	24.22 ± 0.01	22.78 ± 0.03
R32	4	386.9	229.9	12:50:38.77	25:33:18.9	22.40 ± 0.01	22.39 ± 0.01	22.43 ± 0.02	22.48 ± 0.02
R33	4	260.8	239.2	12:50:38.75	25:33:06.3	22.92 ± 0.01	22.04 ± 0.03	22.95 ± 0.02	22.09 ± 0.04
R34	4	394.1	278.2	12:50:39.13	25:33:19.1	24.39 ± 0.01	24.08 ± 0.03	24.39 ± 0.02	24.11 ± 0.02
R35	4	645.0	311.6	12:50:39.55	25:33:43.7	24.76 ± 0.01	24.07 ± 0.21	24.71 ± 0.02	24.33 ± 0.02
R36	4	796.6	348.8	12:50:39.93	25:33:58.3	23.97 ± 0.01	23.07 ± 0.02	23.85 ± 0.02	23.03 ± 0.02
R37	4	636.5	373.0	12:50:39.99	25:33:42.2	24.07 ± 0.01	23.95 ± 0.04	24.15 ± 0.01	24.07 ± 0.06
R38	4	498.9	539.2	12:50:41.12	25:33:27.0	23.72 ± 0.02	23.66 ± 0.06	23.69 ± 0.02	23.74 ± 0.02
R39	4	162.8	525.8	12:50:40.78	25:32:53.8	23.77 ± 0.01	23.60 ± 0.02	23.84 ± 0.03	23.68 ± 0.03
R40	4	202.9	544.6	12:50:40.94	25:32:57.6	20.14 ± 0.01	17.14 ± 0.02	20.29 ± 0.05	17.13 ± 0.03
R41	4	365.6	546.0	12:50:41.07	25:33:13.7	24.33 ± 0.01	23.98 ± 0.04	24.41 ± 0.02	24.08 ± 0.05

Table 2—Continued

ID	Chip	X	Y	RA (J2000)	Dec	ALLFRAME		DoPHOT	
						V	I	V	I
R42	4	287.3	558.0	12:50:41.10	25:33:05.8	23.50 ± 0.01	23.06 ± 0.02	23.56 ± 0.02	23.13 ± 0.03
R43	4	296.4	665.3	12:50:41.90	25:33:05.7	24.46 ± 0.01	24.27 ± 0.04	24.50 ± 0.03	24.36 ± 0.08
R44	4	458.1	671.7	12:50:42.06	25:33:21.7	20.31 ± 0.00	18.76 ± 0.02	20.31 ± 0.03	18.86 ± 0.01
R45	4	305.0	699.0	12:50:42.15	25:33:06.2	22.62 ± 0.01	22.23 ± 0.02	22.59 ± 0.04	22.31 ± 0.03

Table 3. Comparison of ALLFRAME and DoPHOT Magnitudes

Chip	# Stars	ΔV^a	$\sigma_{\Delta V}$	ΔI^a	$\sigma_{\Delta I}$
<i>Reference Stars</i>					
2	17	+0.022	0.073	+0.017	0.050
3	13	-0.045	0.038	-0.030	0.043
4	15	-0.020	0.063	-0.075	0.065
2-4	45	-0.011	0.068	-0.027	0.066
<i>Cepheids</i>					
2	12	+0.088	0.097	+0.038	0.081
3	3	-0.030	0.016	-0.060	0.029
4	5	+0.036	0.055	+0.006	0.042
2-4	20	+0.057	0.091	+0.016	0.075

^a $\Delta \equiv \text{ALLFRAME-DoPHOT}$.

Table 4. Cepheid Candidates Detected in NGC 4725 - Coordinates

ID	Chip	X	Y	RA (J2000)	Dec
C01	2	594.0	100.2	12:50:36.33	25:31:53.5
C02	2	570.6	226.2	12:50:35.42	25:31:56.9
C03	2	523.0	242.7	12:50:35.32	25:32:01.7
C04	2	629.5	336.9	12:50:34.57	25:31:51.9
C05	2	558.8	338.6	12:50:34.60	25:31:58.9
C06	2	675.2	358.3	12:50:34.38	25:31:47.5
C07	2	160.9	473.7	12:50:33.85	25:32:39.5
C08	2	90.3	521.5	12:50:33.54	25:32:46.9
C09	2	183.7	570.6	12:50:33.12	25:32:38.0
C10	2	566.3	585.3	12:50:32.78	25:32:00.2
C11	2	465.9	593.0	12:50:32.79	25:32:10.2
C12	2	97.3	655.6	12:50:32.55	25:32:47.3
C13	3	98.0	230.5	12:50:36.83	25:33:05.5
C14	3	353.9	420.4	12:50:35.08	25:33:26.5
C15	3	674.9	475.8	12:50:32.76	25:33:34.8
C16	4	133.9	230.6	12:50:38.59	25:32:53.8
C17	4	687.7	268.9	12:50:39.27	25:33:48.3
C18	4	724.1	287.8	12:50:39.43	25:33:51.7
C19	4	490.8	333.6	12:50:39.60	25:33:28.2
C20	4	705.9	408.3	12:50:40.30	25:33:48.8

Table 5. Cepheids Detected in NGC 4725 - Properties^a

ID	ALLFRAME/TRIAL			DoPHOT/PDM		
	Period (d)	V	I	Period (d)	V	I
C01	28.95 ± 0.05	25.43 ± 0.03	24.30 ± 0.06	26.9	25.37 ± 0.03	24.39 ± 0.13
C02	12.14 ± 0.02	26.45 ± 0.04	25.30 ± 0.07	12.3	26.25 ± 0.04	25.25 ± 0.07
C03	17.63 ± 0.04	26.01 ± 0.03	24.93 ± 0.05	17.6	25.94 ± 0.04	24.78 ± 0.06
C04	22.19 ± 0.09	25.87 ± 0.03	25.04 ± 0.04	22.2	25.81 ± 0.03	25.08 ± 0.07
C05	28.13 ± 0.28	26.14 ± 0.04	24.93 ± 0.06	29.8	25.91 ± 0.04	24.79 ± 0.05
C06	49.09 ± 0.25	24.86 ± 0.02	23.85 ± 0.03	49.7	24.84 ± 0.02	23.85 ± 0.05
C07	29.63 ± 0.08	25.78 ± 0.02	24.73 ± 0.05	29.4	25.84 ± 0.03	24.74 ± 0.07
C08	31.29 ± 0.45	25.44 ± 0.03	24.39 ± 0.04	33.9	25.44 ± 0.03	24.43 ± 0.05
C09	39.39 ± 0.06	24.85 ± 0.01	23.87 ± 0.02	38.7	24.69 ± 0.01	23.73 ± 0.03
C10	35.46 ± 0.43	24.81 ± 0.02	23.91 ± 0.04	38.1	24.81 ± 0.02	23.94 ± 0.05
C11	22.78 ± 0.02	25.70 ± 0.04	24.66 ± 0.05	22.5	25.44 ± 0.03	24.54 ± 0.05
C12	27.20 ± 0.11	25.87 ± 0.04	24.75 ± 0.06	29.5	25.82 ± 0.03	24.68 ± 0.05
C13	37.63 ± 0.17	25.49 ± 0.02	24.37 ± 0.03	35.8	25.54 ± 0.03	24.47 ± 0.04
C14	17.62 ± 0.15	26.21 ± 0.04	25.22 ± 0.05	17.7	26.24 ± 0.04	25.25 ± 0.07
C15	14.20 ± 0.03	26.36 ± 0.03	25.35 ± 0.05	14.1	26.37 ± 0.04	25.40 ± 0.08
C16	35.93 ± 0.40	25.77 ± 0.02	24.68 ± 0.04	36.1	25.70 ± 0.03	24.66 ± 0.06
C17	31.03 ± 0.12	25.31 ± 0.02	24.23 ± 0.03	31.1	25.24 ± 0.02	24.29 ± 0.05
C18	28.93 ± 0.19	25.47 ± 0.02	24.43 ± 0.04	27.8	25.53 ± 0.02	24.45 ± 0.05
C19	48.41 ± 0.44	25.48 ± 0.02	24.28 ± 0.03	46.2	25.47 ± 0.03	24.22 ± 0.03
C20	13.90 ± 0.03	26.15 ± 0.04	25.36 ± 0.06	14.0	26.06 ± 0.04	25.33 ± 0.07

^aNotes: C01-bright,isolated. C02-faint,isolated. C03-isolated. C04-isolated. C05-bright,neighbor at $\sim 0''.27$. C06-bright,near dust lane. C07-bright,isolated. C08-bright,isolated. C09-bright,isolated. C10-crowded,bright background. C11-isolated,bright background. C12-isolated. C13-bright,isolated. C14-faint,isolated. C15-faint,isolated. C16-isolated. C17-bright,isolated. C18-isolated. C19-isolated. C20-isolated.

Table 6. Measured ALLFRAME Magnitudes and Standard Errors

HJD	Filter	magnitude	magnitude	magnitude	magnitude	magnitude	magnitude
		C01	C02	C03	C04	C05	C06
2449819.813	V	26.16 ± 0.18	27.00 ± 0.40	25.90 ± 0.11	25.68 ± 0.12	26.38 ± 0.22	24.95 ± 0.12
2449819.867	V	26.21 ± 0.17	26.42 ± 0.31	26.05 ± 0.19	25.61 ± 0.17	26.72 ± 0.37	24.99 ± 0.08
2449828.528	V	25.07 ± 0.05	25.65 ± 1.03	26.53 ± 0.19	26.50 ± 0.23	25.76 ± 0.06	25.18 ± 0.12
2449828.579	V	25.22 ± 0.14	25.77 ± 0.14	26.70 ± 0.38	26.29 ± 0.16	25.55 ± 0.13	25.13 ± 0.15
2449828.593	I	23.65 ± 0.41	25.04 ± 0.18	25.34 ± 0.30	25.26 ± 0.26	24.74 ± 0.16	24.11 ± 0.15
2449828.649	I	24.17 ± 0.24	25.12 ± 0.21	25.06 ± 0.19	25.37 ± 0.20	24.85 ± 0.14	23.95 ± 0.11
2449839.777	V	25.67 ± 0.09	26.45 ± 0.16	25.95 ± 0.12	25.60 ± 0.11	26.18 ± 0.20	23.65 ± 0.21
2449839.836	V	25.69 ± 0.19	26.41 ± 0.16	26.30 ± 0.22	25.44 ± 0.11	26.27 ± 0.39	25.07 ± 0.11
2449839.850	I	24.38 ± 0.10	25.95 ± 0.43	24.81 ± 0.17	24.82 ± 0.13	25.39 ± 0.31	23.81 ± 0.06
2449839.907	I	24.77 ± 0.16	25.17 ± 0.20	24.96 ± 0.13	24.98 ± 0.12	25.18 ± 0.27	24.07 ± 0.13
2449842.722	V	24.33 ± 0.44	26.17 ± 0.16	26.46 ± 0.21	25.61 ± 0.14	26.66 ± 0.27	24.81 ± 0.10
2449842.785	V	26.00 ± 0.14	26.25 ± 0.22	26.71 ± 0.35	25.88 ± 0.19	26.26 ± 0.23	24.82 ± 0.10
2449845.269	V	25.98 ± 0.17	26.68 ± 0.18	26.78 ± 0.22	26.05 ± 0.13	26.91 ± 0.30	24.41 ± 0.06
2449845.288	V	26.09 ± 0.20	26.77 ± 0.40	26.48 ± 0.32	26.05 ± 0.21	26.65 ± 0.35	24.59 ± 0.07
2449848.756	V	25.82 ± 0.08	27.23 ± 0.33	25.99 ± 0.12	26.06 ± 0.14	26.68 ± 0.32	24.43 ± 0.05
2449848.819	V	25.91 ± 0.15	27.34 ± 0.47	25.91 ± 0.17	26.01 ± 0.52	26.44 ± 0.33	24.43 ± 0.06
2449852.993	V	24.79 ± 0.07	25.74 ± 0.10	25.90 ± 0.10	24.10 ± 0.22	26.00 ± 0.13	24.62 ± 0.07
2449853.044	V	24.85 ± 0.09	23.29 ± 0.46	24.33 ± 0.65	26.74 ± 0.38	26.32 ± 0.27	23.58 ± 0.35
2449856.946	V	25.07 ± 0.07	26.98 ± 0.34	26.05 ± 0.18	25.82 ± 0.12	25.83 ± 0.15	24.67 ± 0.08
2449856.999	V	25.04 ± 0.10	26.37 ± 0.20	25.95 ± 0.23	25.82 ± 0.19	25.44 ± 0.12	24.81 ± 0.10
2449857.013	I	23.33 ± 0.81	25.41 ± 0.21	24.73 ± 0.12	24.82 ± 0.17	24.57 ± 0.19	23.72 ± 0.08
2449857.069	I	23.47 ± 0.46	25.26 ± 0.17	24.94 ± 0.17	25.15 ± 0.12	24.83 ± 0.13	23.76 ± 0.09
2449857.082	V	25.49 ± 0.25	25.96 ± 0.30	25.95 ± 0.40	26.59 ± 0.75	25.99 ± 0.51	24.76 ± 0.19
2449857.133	I	24.22 ± 0.21	...	24.65 ± 0.30	25.47 ± 0.75	24.35 ± 0.30	23.93 ± 0.18
2449862.174	V	25.43 ± 0.10	27.06 ± 0.35	26.71 ± 0.22	25.62 ± 0.10	25.84 ± 0.12	24.82 ± 0.09
2449862.233	V	24.98 ± 0.64	27.19 ± 0.50	26.42 ± 0.20	25.54 ± 0.10	26.09 ± 0.13	24.74 ± 0.10
2449868.206	V	25.80 ± 0.13	26.56 ± 0.21	25.38 ± 0.10	26.09 ± 0.12	25.48 ± 0.22	24.93 ± 0.08
2449868.264	V	25.78 ± 0.16	26.38 ± 0.23	25.51 ± 0.09	25.99 ± 0.19	25.58 ± 0.16	24.98 ± 0.09
2449874.974	V	26.06 ± 0.15	26.72 ± 0.18	25.78 ± 0.10	26.65 ± 0.33	26.67 ± 0.28	25.10 ± 0.06
2449875.025	V	26.08 ± 0.22	26.97 ± 0.48	26.24 ± 0.35	26.63 ± 0.30	26.67 ± 0.34	25.10 ± 0.10
2449883.417	V	25.00 ± 0.07	26.71 ± 0.17	26.05 ± 0.14	25.47 ± 0.07	25.73 ± 0.11	25.34 ± 0.11
2449883.468	V	24.87 ± 0.07	26.84 ± 0.27	26.41 ± 0.25	25.78 ± 0.20	25.79 ± 0.17	25.21 ± 0.12
2449883.482	I	24.16 ± 0.09	25.17 ± 0.24	24.95 ± 0.21	24.78 ± 0.15	24.78 ± 0.16	24.25 ± 0.11
2449883.538	I	23.86 ± 0.16	25.41 ± 0.22	25.30 ± 0.15	24.86 ± 0.10	24.54 ± 0.12	24.06 ± 0.28
2450203.095	V	24.97 ± 0.09	26.70 ± 0.33	25.47 ± 0.10	26.12 ± 0.17	26.11 ± 0.29	24.75 ± 0.06
2450203.109	V	24.93 ± 0.08	26.73 ± 0.27	25.42 ± 0.13	26.29 ± 0.16	26.20 ± 0.21	24.69 ± 0.06
		C07	C08	C09	C10	C11	C12
2449819.813	V	26.18 ± 0.11	25.64 ± 0.12	24.80 ± 0.06	25.36 ± 0.11	25.30 ± 0.09	26.14 ± 0.17
2449819.867	V	26.23 ± 0.22	25.56 ± 0.11	24.77 ± 0.06	25.44 ± 0.13	23.33 ± 0.27	25.99 ± 0.33
2449828.528	V	26.51 ± 0.19	25.98 ± 0.14	25.12 ± 0.08	24.44 ± 0.06	26.01 ± 0.21	25.47 ± 0.14

Table 6—Continued

HJD	Filter	magnitude	magnitude	magnitude	magnitude	magnitude	magnitude
2449828.579	V	26.92 ± 0.39	26.27 ± 0.23	25.23 ± 0.10	24.33 ± 0.31	26.27 ± 0.51	25.54 ± 0.14
2449828.593	I	25.22 ± 0.23	24.69 ± 0.16	23.97 ± 0.09	23.64 ± 0.13	24.83 ± 0.13	24.57 ± 0.11
2449828.649	I	25.06 ± 0.30	24.90 ± 0.16	23.88 ± 0.08	23.57 ± 0.05	25.05 ± 0.18	24.56 ± 0.13
2449839.777	V	25.66 ± 0.11	25.05 ± 0.08	25.16 ± 0.09	24.69 ± 0.08	25.03 ± 0.08	25.96 ± 0.17
2449839.836	V	25.56 ± 0.13	25.13 ± 0.08	25.18 ± 0.08	24.91 ± 0.12	25.21 ± 0.10	26.41 ± 0.38
2449839.850	I	24.50 ± 0.13	24.27 ± 0.10	24.09 ± 0.10	23.78 ± 0.10	24.54 ± 0.17	22.93 ± 0.34
2449839.907	I	24.62 ± 0.11	24.14 ± 0.07	24.17 ± 0.11	23.79 ± 0.09	24.35 ± 0.09	24.82 ± 0.13
2449842.722	V	25.69 ± 0.13	25.27 ± 0.08	24.78 ± 0.07	25.04 ± 0.10	24.39 ± 0.27	26.66 ± 0.21
2449842.785	V	25.77 ± 0.14	25.31 ± 0.11	24.76 ± 0.09	24.99 ± 0.12	25.38 ± 0.14	26.43 ± 0.29
2449845.269	V	25.70 ± 0.10	24.83 ± 0.33	24.38 ± 0.05	24.91 ± 0.07	25.54 ± 0.08	26.29 ± 0.22
2449845.288	V	25.23 ± 1.11	25.51 ± 0.17	24.41 ± 0.06	24.88 ± 0.07	25.65 ± 0.13	26.36 ± 0.30
2449848.756	V	26.19 ± 0.14	25.59 ± 0.10	24.44 ± 0.06	25.04 ± 0.10	25.95 ± 0.13	26.14 ± 0.17
2449848.819	V	26.06 ± 0.17	25.57 ± 0.09	24.47 ± 0.08	24.91 ± 0.09	25.66 ± 0.13	26.17 ± 0.29
2449852.993	V	26.64 ± 0.22	24.09 ± 0.26	24.61 ± 0.06	25.12 ± 0.11	25.39 ± 0.73	24.22 ± 0.60
2449853.044	V	26.52 ± 0.15	25.77 ± 0.29	24.75 ± 0.08	25.35 ± 0.14	25.96 ± 0.17	25.47 ± 0.09
2449856.946	V	26.27 ± 0.21	25.92 ± 0.22	24.82 ± 0.06	25.37 ± 0.12	26.28 ± 0.17	25.59 ± 0.16
2449856.999	V	26.38 ± 0.26	26.24 ± 0.18	24.71 ± 0.09	25.36 ± 0.14	25.90 ± 0.21	25.60 ± 0.15
2449857.013	I	25.06 ± 0.39	24.74 ± 0.12	23.77 ± 0.06	24.46 ± 0.16	24.70 ± 0.14	24.82 ± 0.17
2449857.069	I	25.24 ± 0.23	25.00 ± 0.18	23.76 ± 0.08	24.29 ± 0.11	24.52 ± 0.34	24.56 ± 0.14
2449857.082	V	25.89 ± 0.41	26.77 ± 0.95	24.64 ± 0.18	25.28 ± 0.34	26.62 ± 1.05	25.60 ± 0.24
2449857.133	I	24.81 ± 0.30	24.78 ± 0.49	23.79 ± 0.16	24.50 ± 0.31	26.53 ± 0.78	25.05 ± 0.28
2449862.174	V	25.46 ± 0.11	25.88 ± 0.13	24.88 ± 0.05	24.76 ± 0.14	25.17 ± 0.12	25.97 ± 0.13
2449862.233	V	25.34 ± 0.11	25.98 ± 0.18	24.79 ± 0.08	24.73 ± 0.06	25.07 ± 0.09	25.94 ± 0.16
2449868.206	V	25.40 ± 0.09	24.83 ± 0.06	25.18 ± 0.09	24.42 ± 0.04	25.70 ± 0.07	23.55 ± 0.24
2449868.264	V	25.40 ± 0.22	24.74 ± 0.08	25.11 ± 0.11	24.46 ± 0.05	25.55 ± 0.12	26.31 ± 0.24
2449874.974	V	26.02 ± 0.13	25.18 ± 0.09	25.45 ± 0.08	24.67 ± 0.08	26.22 ± 0.13	26.31 ± 0.17
2449875.025	V	25.83 ± 0.17	25.11 ± 0.14	25.56 ± 0.11	24.65 ± 0.05	26.23 ± 0.23	25.79 ± 0.15
2449883.417	V	26.40 ± 0.22	25.75 ± 0.13	24.48 ± 0.06	24.94 ± 0.10	25.14 ± 0.49	25.49 ± 0.13
2449883.468	V	26.27 ± 0.16	25.36 ± 0.20	24.58 ± 0.08	25.05 ± 0.15	25.58 ± 0.13	25.59 ± 0.14
2449883.482	I	25.17 ± 0.19	24.56 ± 0.12	23.71 ± 0.06	23.95 ± 0.11	24.55 ± 0.10	24.42 ± 0.13
2449883.538	I	24.99 ± 0.19	24.43 ± 0.15	23.69 ± 0.06	22.87 ± 0.42	24.66 ± 0.09	24.81 ± 0.14
2450203.095	V	26.22 ± 0.20	26.04 ± 0.17	24.40 ± 0.05	25.30 ± 0.13	25.35 ± 0.09	25.93 ± 0.20
2450203.109	V	25.98 ± 0.15	26.12 ± 0.19	24.40 ± 0.08	25.06 ± 0.15	25.24 ± 0.08	26.44 ± 0.25
		C13	C14	C15	C16	C17	
2449819.813	V	25.35 ± 0.39	26.14 ± 0.33	26.67 ± 0.29	25.19 ± 0.07	25.47 ± 0.12	25.82 ± 0.11
2449819.867	V	25.62 ± 0.17	26.15 ± 0.24	26.79 ± 0.38	25.33 ± 0.10	25.68 ± 0.18	25.92 ± 0.18
2449828.528	V	25.71 ± 0.14	26.35 ± 0.20	25.95 ± 0.16	25.73 ± 0.11	26.04 ± 0.20	25.96 ± 0.10
2449828.579	V	25.84 ± 0.17	23.33 ± 0.56	25.98 ± 0.16	25.83 ± 0.17	25.88 ± 0.11	25.04 ± 0.89
2449828.593	I	24.69 ± 0.18	25.64 ± 0.27	25.05 ± 0.20	24.57 ± 0.19	24.67 ± 0.12	24.77 ± 0.69
2449828.649	I	24.71 ± 0.11	25.57 ± 0.21	25.12 ± 0.14	24.38 ± 0.15	24.70 ± 0.08	24.95 ± 0.10
2449839.777	V	25.18 ± 0.10	25.82 ± 0.14	26.42 ± 0.15	26.08 ± 0.09	24.89 ± 0.07	25.27 ± 0.10

Table 6—Continued

HJD	Filter	magnitude	magnitude	magnitude	magnitude	magnitude	magnitude
2449839.836	V	25.24 ± 0.11	25.55 ± 0.11	26.49 ± 0.22	26.20 ± 0.18	24.93 ± 0.09	25.38 ± 0.22
2449839.850	I	24.25 ± 0.09	24.91 ± 0.12	25.17 ± 0.18	24.93 ± 0.17	23.99 ± 0.10	24.34 ± 0.12
2449839.907	I	24.41 ± 0.09	24.88 ± 0.12	25.44 ± 0.25	24.70 ± 0.12	24.01 ± 0.08	24.21 ± 0.05
2449842.722	V	25.14 ± 0.08	26.00 ± 0.16	25.88 ± 0.14	26.14 ± 0.13	25.12 ± 0.08	25.76 ± 0.08
2449842.785	V	25.02 ± 0.09	25.88 ± 0.13	25.58 ± 0.10	26.22 ± 0.25	25.12 ± 0.09	25.60 ± 0.14
2449845.269	V	25.21 ± 0.10	26.28 ± 0.15	26.30 ± 0.14	25.95 ± 0.16	25.21 ± 0.08	25.80 ± 0.12
2449845.288	V	25.07 ± 0.11	26.41 ± 0.40	26.20 ± 0.19	26.34 ± 0.24	25.14 ± 0.11	25.56 ± 0.07
2449848.756	V	25.40 ± 0.11	26.57 ± 0.16	26.60 ± 0.20	26.09 ± 0.16	25.40 ± 0.08	26.00 ± 0.14
2449848.819	V	25.30 ± 0.05	26.99 ± 0.38	27.21 ± 0.40	26.01 ± 0.22	25.43 ± 0.13	25.42 ± 0.35
2449852.993	V	25.51 ± 0.09	26.66 ± 0.29	26.63 ± 0.22	25.52 ± 0.13	25.71 ± 0.09	26.02 ± 0.17
2449853.044	V	25.60 ± 0.15	26.36 ± 0.21	26.83 ± 0.33	25.47 ± 0.10	24.64 ± 0.40	25.86 ± 0.10
2449856.946	V	25.58 ± 0.15	25.53 ± 0.11	26.06 ± 0.16	25.41 ± 0.09	25.80 ± 0.09	25.93 ± 0.08
2449856.999	V	25.61 ± 0.14	25.70 ± 0.13	25.84 ± 0.14	25.38 ± 0.09	25.69 ± 0.15	26.29 ± 0.19
2449857.013	I	24.29 ± 0.11	24.84 ± 0.16	25.00 ± 0.21	24.39 ± 0.14	24.48 ± 0.09	24.75 ± 0.13
2449857.069	I	24.38 ± 0.11	24.94 ± 0.14	25.41 ± 0.16	24.51 ± 0.08	24.56 ± 0.09	24.72 ± 0.18
2449857.082	V	25.65 ± 0.33	25.99 ± 0.46	25.85 ± 0.41	25.21 ± 0.13	21.94 ± 0.36	25.81 ± 0.41
2449857.133	I	24.67 ± 0.42	25.32 ± 0.57	24.92 ± 0.35	25.23 ± 0.74	24.91 ± 0.32	25.27 ± 0.45
2449862.174	V	25.75 ± 0.14	26.42 ± 0.18	26.66 ± 0.32	25.51 ± 0.09	25.72 ± 0.09	24.84 ± 0.06
2449862.233	V	25.78 ± 0.17	26.28 ± 0.28	26.77 ± 0.34	25.56 ± 0.12	25.75 ± 0.70	24.80 ± 0.07
2449868.206	V	25.85 ± 0.15	26.67 ± 0.56	26.59 ± 0.15	25.86 ± 0.14	24.64 ± 0.07	25.30 ± 0.08
2449868.264	V	25.85 ± 0.16	26.77 ± 0.30	26.51 ± 0.24	25.56 ± 0.29	24.70 ± 0.07	25.29 ± 0.09
2449874.974	V	25.47 ± 0.13	25.71 ± 0.12	26.42 ± 0.25	26.14 ± 0.14	25.11 ± 0.08	25.60 ± 0.12
2449875.025	V	25.47 ± 0.15	25.75 ± 0.13	26.25 ± 0.20	26.14 ± 0.14	25.16 ± 0.08	25.69 ± 0.10
2449883.417	V	25.05 ± 0.57	25.97 ± 0.47	26.10 ± 0.14	26.12 ± 0.17	25.59 ± 0.11	26.02 ± 0.13
2449883.468	V	25.22 ± 0.09	26.92 ± 0.27	26.20 ± 0.22	26.06 ± 0.22	25.59 ± 0.13	25.73 ± 0.12
2449883.482	I	24.07 ± 0.08	25.26 ± 0.35	25.64 ± 0.33	25.19 ± 0.22	24.36 ± 0.09	24.65 ± 0.13
2449883.538	I	24.18 ± 0.09	25.42 ± 0.20	25.19 ± 0.21	25.31 ± 0.18	23.07 ± 0.31	24.81 ± 0.10
2450203.095	V	25.79 ± 0.11	26.62 ± 0.38	26.53 ± 0.22	26.23 ± 0.16	25.88 ± 0.14	26.00 ± 0.14
2450203.109	V	25.69 ± 0.12	27.22 ± 0.37	26.96 ± 0.28	26.27 ± 0.25	25.75 ± 0.12	26.15 ± 0.24
		C19	C20				
2449819.813	V	25.35 ± 0.08	26.47 ± 0.18				
2449819.867	V	25.32 ± 0.10	26.93 ± 0.39				
2449828.528	V	25.57 ± 0.08	26.08 ± 0.11				
2449828.579	V	25.55 ± 0.16	26.13 ± 0.19				
2449828.593	I	22.99 ± 0.34	25.06 ± 0.16				
2449828.649	I	24.30 ± 0.06	25.48 ± 0.19				
2449839.777	V	25.76 ± 0.14	25.78 ± 0.15				
2449839.836	V	25.58 ± 0.12	25.84 ± 0.14				
2449839.850	I	24.32 ± 0.13	25.27 ± 0.21				
2449839.907	I	24.29 ± 0.09	25.47 ± 0.21				
2449842.722	V	25.90 ± 0.14	26.35 ± 0.17				

Table 6—Continued

HJD	Filter	magnitude	magnitude	magnitude	magnitude	magnitude	magnitude
2449842.785	V	25.76 ± 0.15	26.12 ± 0.20				
2449845.269	V	25.77 ± 0.16	26.44 ± 0.13				
2449845.288	V	25.77 ± 0.18	26.50 ± 0.22				
2449848.756	V	25.67 ± 0.14	26.58 ± 0.19				
2449848.819	V	25.43 ± 0.10	26.84 ± 0.28				
2449852.993	V	25.43 ± 0.13	25.50 ± 0.09				
2449853.044	V	25.53 ± 0.11	25.59 ± 0.11				
2449856.946	V	25.27 ± 0.07	26.16 ± 0.11				
2449856.999	V	24.09 ± 0.45	25.91 ± 0.15				
2449857.013	I	24.18 ± 0.07	25.25 ± 0.19				
2449857.069	I	24.15 ± 0.07	25.22 ± 0.14				
2449857.082	V	25.92 ± 0.41	26.60 ± 0.53				
2449857.133	I	24.32 ± 0.17	26.06 ± 1.41				
2449862.174	V	25.26 ± 0.08	26.65 ± 0.19				
2449862.233	V	25.16 ± 0.08	26.58 ± 0.24				
2449868.206	V	25.30 ± 0.10	25.85 ± 0.11				
2449868.264	V	25.45 ± 0.14	26.02 ± 0.13				
2449874.974	V	25.53 ± 0.11	26.40 ± 0.23				
2449875.025	V	25.36 ± 0.11	26.81 ± 0.47				
2449883.417	V	25.66 ± 0.11	26.03 ± 0.13				
2449883.468	V	25.59 ± 0.16	26.29 ± 0.16				
2449883.482	I	24.32 ± 0.10	25.09 ± 0.19				
2449883.538	I	24.42 ± 0.08	25.21 ± 0.22				
2450203.095	V	25.30 ± 0.10	23.73 ± 0.52				
2450203.109	V	25.36 ± 0.10	26.04 ± 0.14				

Table 7. ALLFRAME Error Budget

Source of Uncertainty	Error (mag)	Notes
CEPHEID PL CALIBRATION		
(a) LMC True Modulus	± 0.10	(1)
(b) V PL Zero Point	± 0.05	(2),(3)
(c) I PL Zero Point	± 0.03	(2),(4)
(S1) PL Systematic Uncertainty	± 0.12	(a),(b),(c) combined in quadrature
NGC 4725 MODULUS		
(d) HST V-Band Zero Point	± 0.05	(5)
(e) HST I-Band Zero Point	± 0.05	(5)
(R1) Cepheid True Modulus	± 0.15	(6)
(R2) Dereddened PL Fit	± 0.06	(7)
(S2) Metallicity Uncertainty	$+0.12 \pm 0.21$	See text for details
TOTAL UNCERTAINTY		
(R) Random Errors	± 0.16	(R1),(R2) combined in quadrature
(S) Systematic Errors	± 0.17	(S1),(S2) combined in quadrature

(1) Adopted from Madore & Freedman (1991). (2) Derived from the observed scatter in the Madore & Freedman (1991) PL relation, with 32 contributing Cepheids. (3) V-band 1σ scatter: ± 0.27 mag. (4) I-band 1σ scatter: ± 0.18 mag. (5) Contributing uncertainties from aperture corrections, the Holtzmann et al. (1995) zero points, and the long versus short uncertainty, combined in quadrature. Adopted aperture correction contribution is the worst-case formal uncertainty (± 0.04 mag) for the NGC 4725 aperture corrections. Adopted Holtzmann et al. zero point uncertainty is ± 0.02 mag. Adopted long versus short exposure correction uncertainty is ± 0.02 mag. (6) Assuming that photometric errors (d,e) are uncorrelated between filters, and noting that that V and I magnitudes are multiplied by +1.45 and -2.45, respectively, when correcting for reddening, results in a derived error on the true modulus of $[(1.45)^2(0.05)^2 + (-2.45)^2(0.05)^2]^{1/2} = 0.15$ mag. (7) Uncertainties for the mean true modulus result from the finite width of the instability strip and the random star-to-star photometric errors, reduced by the population size of contributing Cepheids for NGC 4725 (20 variables).

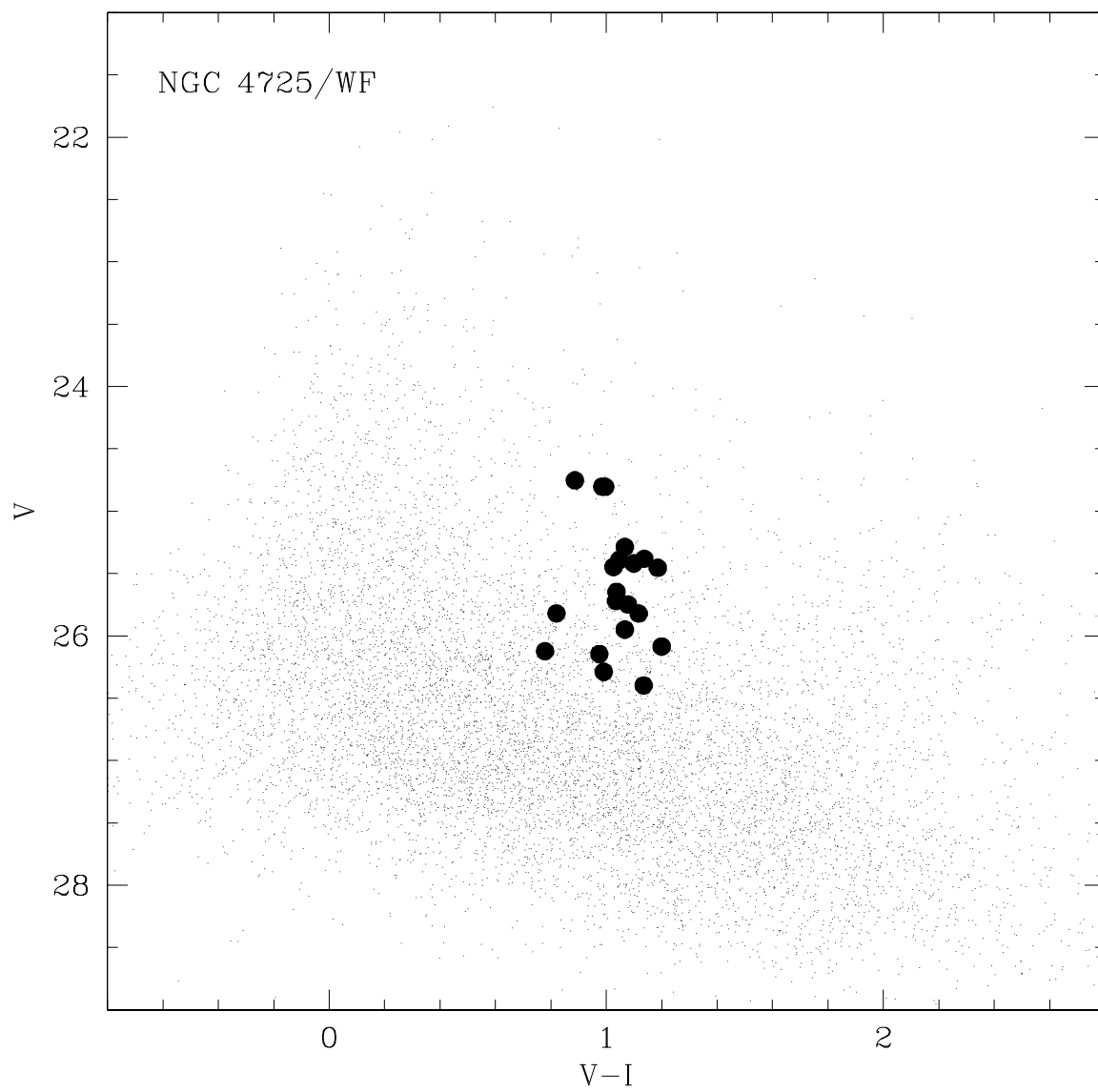
Table 8. Published Distances to NGC 4725 and the Coma Cloud^a

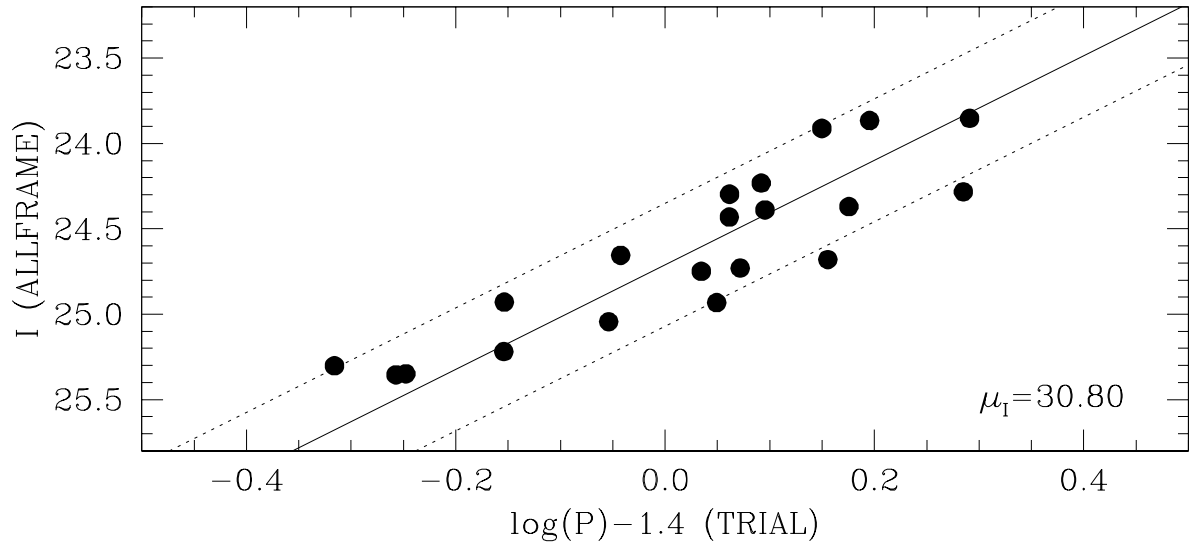
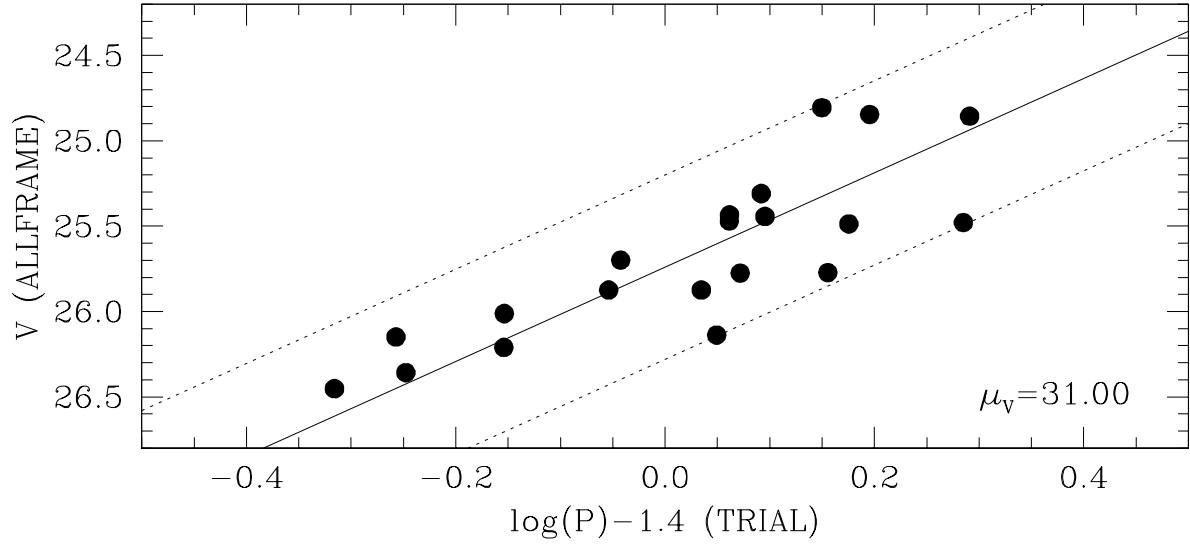
Method	Distance (Mpc)	Reference
<i>NGC 4725</i>		
TF (B-band)	9.9 ± 1.0	Bottinelli et al. (1985)
Mass Model	12.4	Tully (1988)
TF (H-band)	16.1	Tully et al. (1992)
Mass Model	20	Tully et al. (1992)
TF (BRIH-band)	12.6 ± 2.1	Tully (1997)
SBF	13.1 ± 2.2	Tonry (1998)
Cepheids	12.6 ± 1.0	This paper (ALLFRAME)
<i>NGC 4414</i>		
Cepheids	19.1 ± 1.6	Turner et al. (1998)
<i>NGC 4278</i>		
GCLF ^b	13.2 ± 0.9	Forbes (1996)
PNLF	10.2 ± 1.0	Jacoby et al. (1996)
<i>NGC 4494</i>		
Mass Model	11.7	Tully & Shaya (1984)
SBF	15.0 ± 2.3	Simard & Pritchet (1994)
GCLF ^b	14.5 ± 2.9	Fleming et al. (1995)
GCLF ^b	12.6 ± 0.9	Forbes (1996)
PNLF	12.8 ± 0.9	Jacoby et al. (1996)
<i>NGC 4565</i>		
Mass Model	11.0	Tully & Shaya (1984)
SBF	10.4 ± 0.4	Simard & Pritchet (1994)
GCLF ^b	10.0 ± 1.5	Fleming et al. (1995)
PNLF	10.5 ± 1.0	Jacoby et al. (1996)
<i>Average of NGC 4150,4251,4283</i>		
SBF	15.5 ± 0.6	Tonry et al. (1997)
<i>Average of NGC 4494,4565,4725</i>		
SBF ^c	15.9 ± 0.6	Tonry et al. (1997)

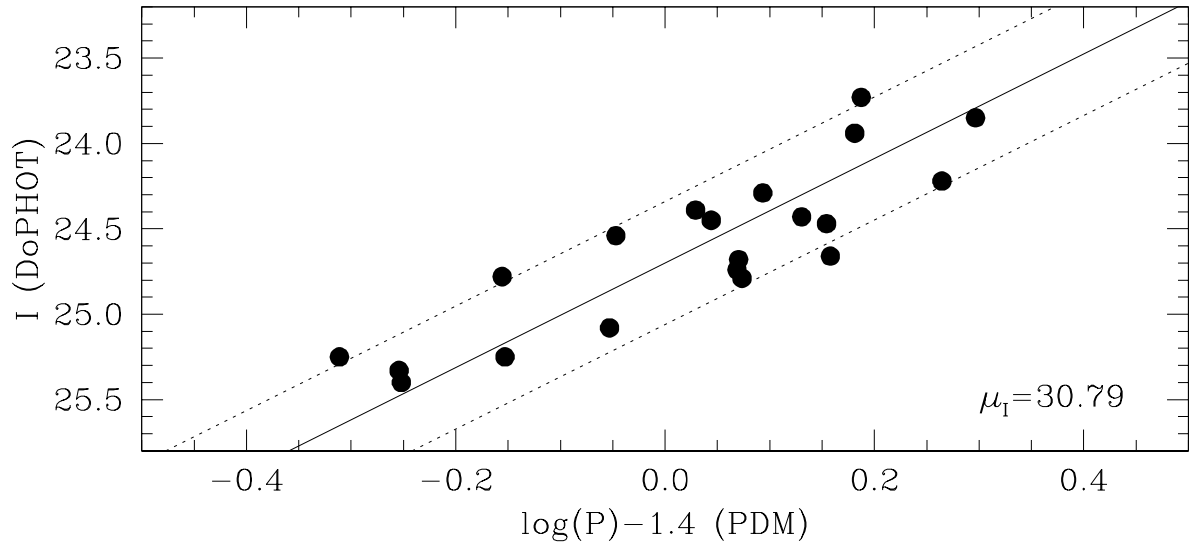
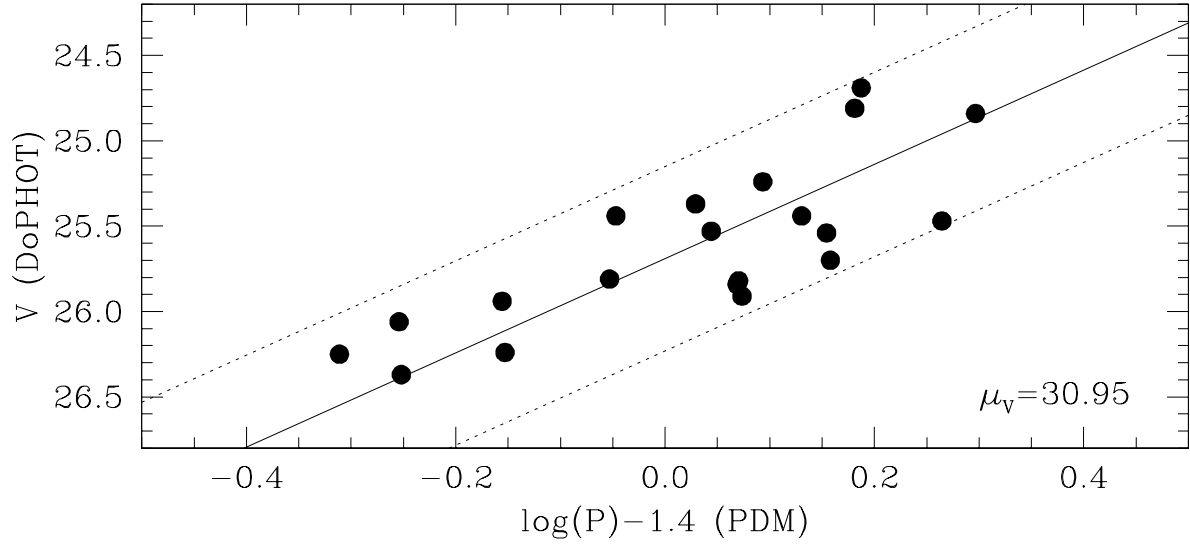
^aFor convenience, the presented Coma Cloud inventory follows that of Tully (1988) - i.e. his Groups 14-1 (Coma I) and 14-2 (Coma II), respectively, from his Table II. The complexity of this region makes any unequivocal claim of a true physical association between *all* (or, arguably, any) of the listed Coma Cloud “members” highly suspect.

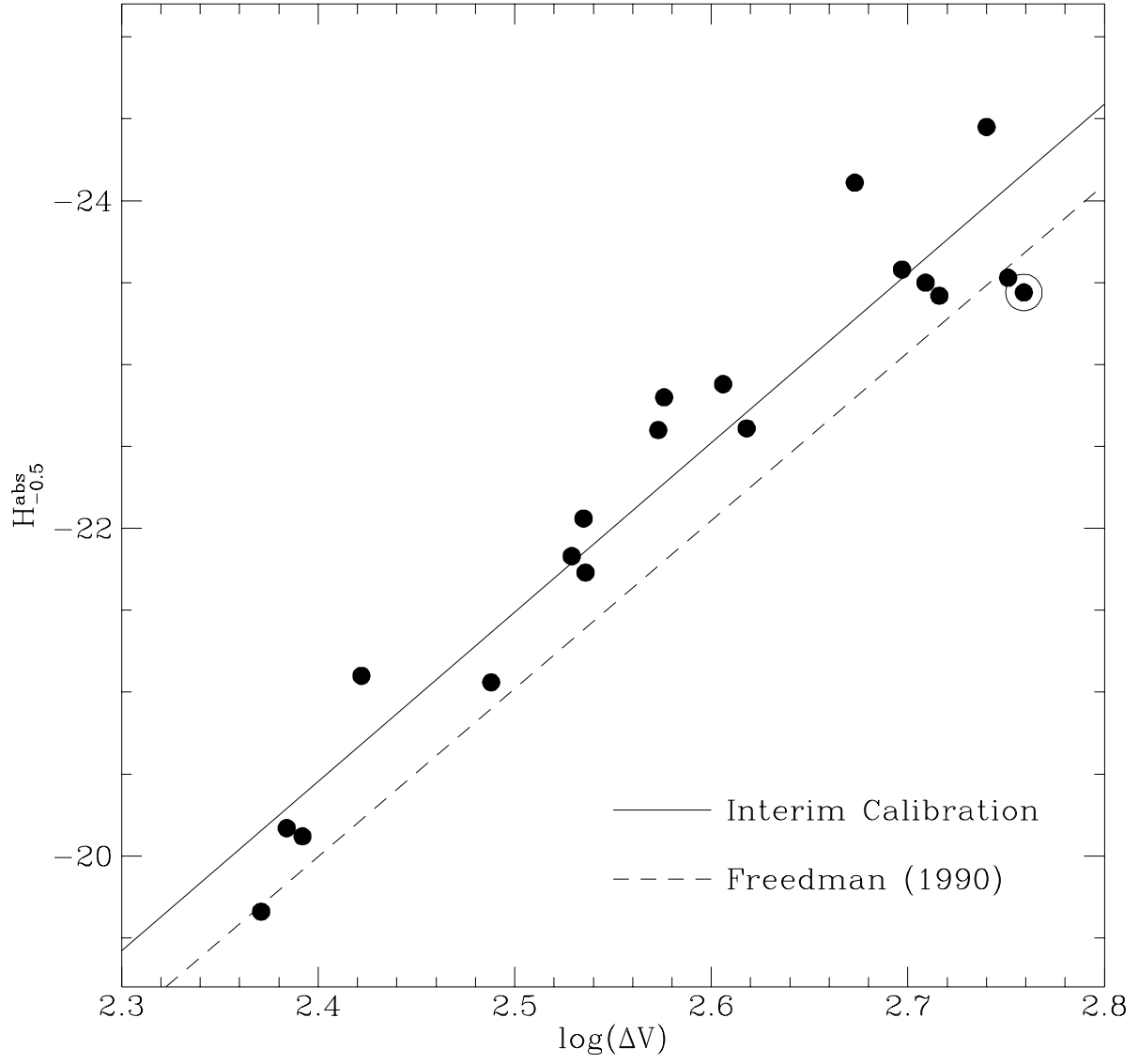
^bFleming et al.’s (1995) results are based upon ground-based CFHT data, whereas Forbes (1996) used *HST*. The latter reference revisits Fleming et al.’s conclusions, in light of the *HST* results.

^cTonry et al. (1997) compute a Coma II Group distance based upon the (approximate) mean of the SBF distances to NGC 4494, 4565, and 4725 (Tonry 1998). Tully’s (1988) inventory would place NGC 4494 and 4565 in the Coma I Group, with only NGC 4725 *strictly* a Coma II Group member.









This figure "f1.jpg" is available in "jpg" format from:

<http://arxiv.org/ps/astro-ph/9810003v1>

This figure "f2a.jpg" is available in "jpg" format from:

<http://arxiv.org/ps/astro-ph/9810003v1>

This figure "f2b.jpg" is available in "jpg" format from:

<http://arxiv.org/ps/astro-ph/9810003v1>

This figure "f2c.jpg" is available in "jpg" format from:

<http://arxiv.org/ps/astro-ph/9810003v1>

This figure "f3.jpg" is available in "jpg" format from:

<http://arxiv.org/ps/astro-ph/9810003v1>

This figure "f4a.jpg" is available in "jpg" format from:

<http://arxiv.org/ps/astro-ph/9810003v1>

This figure "f4b.jpg" is available in "jpg" format from:

<http://arxiv.org/ps/astro-ph/9810003v1>

This figure "f4c.jpg" is available in "jpg" format from:

<http://arxiv.org/ps/astro-ph/9810003v1>

This figure "f4d.jpg" is available in "jpg" format from:

<http://arxiv.org/ps/astro-ph/9810003v1>